ISSN 1807-1929
Revista Brasileira de Engenharia Agrícola e Ambiental
Brazilian Journal of Agricultural and Environmental Engineering
v.30, n.2, e295785, 2026
Campina Grande, PB – http://www.agriambi.com.br – http://www.scielo.br/rbeaa

Original Article

Design and testing of a liquid-flow-assisted seed guiding device for soybean precision planters[1]

Projeto e teste de um dispositivo de orientação de sementes assistido por fluxo de líquido para semeadoras de precisão de soja

Xiaomeng Xia[2,3,4], Jian Wang[2], Jinhui Zhao[5] & Mingwei Li[2,3,4*]

[1] Research developed at Shandong University of Technology, Zibo, Shandong, China
[2] Shandong University of Technology/School of Agricultural Engineering and Food Science, Zibo, China
[3] Shandong University of Technology/Institute of Modern Agricultural Equipment, Zibo, China
[4] Shandong Provincial Key Laboratory of Smart Agricultural Technology and Intelligent Farm Machinery Equipment for Field Crops, Zibo, China
[5] State Key Laboratory of Agricultural Equipment Technology, Beijing, China

HIGHLIGHTS:

A liquid flow-assisted seed guiding device use forward liquid flow to reduce seed collisions within the seed guiding tube.
The seed guiding angle, seeding rotation speed, and flow rate are key factors affecting performance of the device.
The device increases the qualified seed spacing rate by 7.7% and reduces the coefficient of variation by 10.98%.

ABSTRACT: During precision sowing, seeds have disorderly collisions within the seed guiding tube, leading to a reduction in spacing uniformity. To address this issue, a liquid-flow-assisted seed guiding device was designed to reduce the collision of seeds in the seed guiding tube by using forward liquid flow, thereby improving the uniformity of plant spacing. Analysis of the seed delivery process identified three primary factors that influence sowing uniformity under liquid-assisted conditions: the seed guiding angle, the seeding rotation speed, and the flow rate. Indoor experiments were carried out with these three key factors as independent variables, and the qualified rate of seed spacing and the coefficient of variation were used as performance evaluation metrics. The optimal parameter combination was determined to be a seed guiding angle of 10°, a seeding rotation speed of 33.3 rpm, and a flow rate of 800 mL min^{-1}. A validation test revealed that, compared with a conventional seed guide tube, the proposed device increased the qualified rate of seed spacing by 7.7% and reduced the coefficient of variation by 10.98% at a forward speed of 10 km h^{-1}. These findings offer a valuable reference and technical foundation for the innovative design of seed guiding systems.

Key words: *Glycine max*, liquid-assisted seed guidance, precision seeding uniformity, V-shaped guiding tube, agricultural machinery

RESUMO: Durante a semeadura de precisão, as sementes apresentam colisões desordenadas dentro do tubo guia da semente, levando a uma redução na uniformidade do espaçamento. Para resolver esse problema, um dispositivo de orientação de sementes assistido por fluxo de líquido foi projetado para reduzir a colisão de sementes no tubo de orientação de sementes, utilizando fluxo de líquido de fluxo para frente, melhorando assim a uniformidade do espaçamento entre as plantas. A análise do processo de entrega de sementes identificou três fatores principais que influenciam a uniformidade da semeadura em condições assistidas por líquido: o ângulo de orientação da semente, a velocidade de rotação da semeadura e a vazão. Experimentos internos foram realizados com esses três fatores-chave como variáveis independentes, e a taxa de espaçamentos qualificados entre sementes e o coeficiente de variação foram usados como métricas de avaliação de desempenho. A combinação ideal de parâmetros foi determinada como um ângulo de orientação da semente de 10°, uma velocidade de rotação de semeadura de 33,3 rpm e uma vazão de 800 mL min^{-1}. Um teste de validação revelou que, em comparação com um tubo-guia de sementes convencional, o dispositivo proposto aumentou a taxa qualificada de espaçamento de sementes em 7,7% e reduziu o coeficiente de variação em 10,98% a uma velocidade de avanço de 10 km h^{-1}. Essas descobertas oferecem uma referência valiosa e uma base técnica para o desenho inovador de sistemas de orientação de sementes.

Palavras-chave: *Glycine max*, fluxo de sementes assistido por líquido, uniformidade na semeadura de precisão, tubo guia em formato de V, máquinas agrícolas

• Ref. 295785 – Received 07 Apr, 2025
* Corresponding author - E-mail: 17866788583@163.com
• Accepted 09 Sept, 2025 • Published 18 Sept, 2025
Editors: Ítalo Herbet Lucena Cavalcante & Walter Esfrain Pereira

Introduction

The key to precision seeding lies in optimising the precision seed discharge system (Ren et al., 2024). At present, seed metering device technology is relatively mature and can realise high-precision single seeding, so it is necessary to optimise the seed guidance system (Gai et al., 2023). There are two main approaches to enhance the existing seed guide technology. The first approach is based on the principle of zero speed seeding (Chen et al., 2023). With this approach, the reverse speed is used to offset the forward speed of the machine so that the seed lands smoothly. The second approach is to constrain the seed trajectory through the seed guide device to reduce the height and randomness of seeding.

There has been extensive research on seed guidance technology and devices (Carpes et al., 2017; Kumar & Raheman, 2018; Hou et al., 2020; Liao et al., 2020). Endrerud et al. (1999) examined the geometric parameters of the seed guiding tube and confirmed that a 45° inclination angle does not affect energy loss in the seed guiding tube. Kocher et al. (2011) used the smoothness of the old and new seed guides as a factor in their study and found that smoother seed guides improve seeding accuracy by more than 20%. Yazgi (2016) compared the seeding performance of plastic corrugated seed guides, plain seed guides, and metal smooth-surface seed guides by considering the material and size and shape of the seed guides. They used the seeding pass rate as an indicator and found that a metal seed guide with a smooth surface provides better seeding performance than a plastic seed guide. Wang et al. (2010) photographed the movement trajectory of corn seeds in a seed guiding tube with the help of a high-speed camera and studied the first landing point and movement trajectory of corn seeds falling into the seed guiding tube at different rotational speeds. The study showed that the difference in the rotational speed of the seed metering device results in a lateral offset of falling seeds. Li et al. (2024b) based their work on the theory of zero-speed seed casting. They leveraged the response surface methodology (RSM) optimisation module within the Isight software to identify the optimal seed guiding tube curve, using the coefficient of variation of plant spacing and the horizontal speed at exit as the evaluation criteria. Dong et al. (2023) designed a new type of guided seed delivery mechanism to improve high-speed sowing of a maize attitude-controlled, drive-guided seed metering by precisely controlling the seed casting trajectory, seed casting point, and initial speed. They designed a two-stage seed guiding tube connected to a rotating vice that could carry out overall translation and rotational movement around the rotating vice under the action of the driving mechanism (Chen et al., 2022). Based on the Venturi principle, Liu et al. (2023b) designed a seed-guiding device that utilises positive pressure airflow to assist in seed delivery. It shows superior performance under high-speed operating conditions.

Although existing research has reduced the degree of seed bouncing, it has not yet identified a way to avoid the collision bouncing problem due to direct contact between a seed and a seed guide tube. Thus, the present study involved the design of a liquid-flow-assisted seed guiding device utilising forward liquid flow to reduce seed collision in the seed guide tube and to improve spacing uniformity.

Material and Methods

Figure 1 presents the working principle of the liquid-flow-assisted seed guiding device for precise soybean planting. The experiment was conducted in August 2023 at the Modern Agricultural Equipment Laboratory of Shandong University of Science and Technology, China (118° 00’ 19.56″ E, 36° 48’ 18.18″ N, altitude 38.3 m).

During operation, the brush-type soybean seed metering device uses brushes in the seeding area to ensure that the seeds are discharged into the disc-shaped holes in the seed port and thus do not fall into the inner cavity of the device. The peristaltic pump delivers liquid smoothly to the seed guiding tube via a silicone hose, with an impulse buffer at the inlet to reduce flow fluctuations. The liquid, specifically water, forms a film along the tube wall, cushioning the seeds at an angle as they enter from the metering device. This reduces collisions and offsets during descent, ensuring stable and uniform seed delivery (Zhu et al., 2023).

As shown in Figure 2, the upper part of the seed guiding tube has an inclined linear shape, serving as a buffer zone for

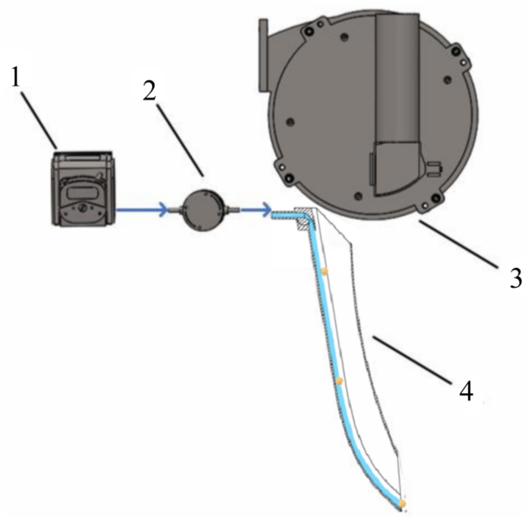

1 - Peristaltic pump; 2 - Pulse damper; 3 - Seed-metering device; 4 - Seed guiding tube

Figure 1. A diagram of the liquid-flow-assisted seed guiding device

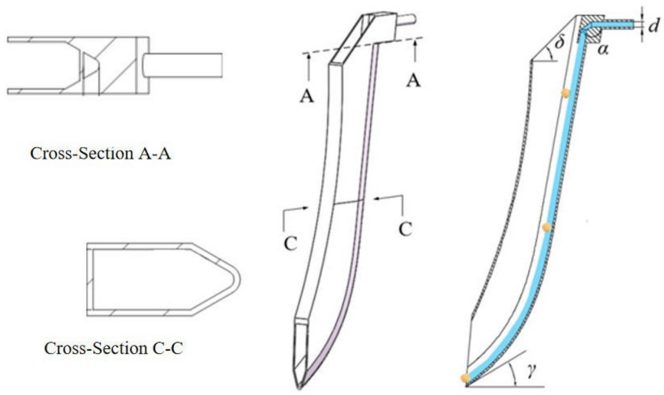

α - Angle of the inclined flow channel, °; d - Liquid flow inlet diameter, mm; γ - Seeding angle, °; δ - Liquid inlet angle, °

Figure 2. A schematic of the seed guiding tube structure

liquid flow. The lower part is parabolic in shape, providing the seed with horizontal velocity to counteract the forward motion of the planter. Based on the positional relationship between a conventional seed metering device and the opener, the height of the seed guiding tube is 450 mm. To minimise the seed velocity as it exits the guiding tube, the straight section has a height of 200 mm and the parabolic section has a height of 250 mm. The lower end of the parabolic curve is tangent to the seed casting point at a seeding angle γ, and the top of the curve is tangent to the straight section. According to the conventional seed guiding tube design, the casting angle is typically 25°-40°; these values are used in the present numerical study.

The width of the seed guide tube slot was calculated according to the width of the soybeans (Eq. 1). Three commonly used soybean varieties in the Yellow and Huaihai regions of China (Zhonghuang No. 37, Qihuang No. 34, and Zheng 1307) were selected for the study. This approach helped to adapt the device to different seed varieties. One hundred intact soybean seeds were randomly selected and their width and thickness were measured using a digital vernier calliper. The measured width was 6.2-7.12 mm and the thickness was 4.18-7.02 mm. Thus, the seed guiding tube cross-section width was 24 mm.

$$4.1\overline{w} \geq W \geq 3.4\overline{w} \tag{1}$$

where:

$\overline{w}$ - average seed width, mm; and,

W - cross-sectional width of the seed guiding tube, mm.

The cross-section of the seed guide tube was designed as a V-shaped groove to ensure the convergence of the liquid flow within the seed guiding tube. This design ensured convergence of the liquid flow in the seed guiding tube at an angle (θ) of 150°. The V-shaped groove exceeded the maximum size of the seed, so the radius of the V-shaped groove fillet was designed to be 10 mm (Xue et al., 2020).

The inlet diameter of the liquid flow directly affects flow velocity and thickness within the seed guiding tube, which in turn determines its buffering and transport capacity. Based on the 10-mm arc radius of the V-shaped groove and the structural constraints of connected components, an inlet diameter (d) of 5-8 mm was determined to be appropriate.

To facilitate a smooth transition from the circular inlet to the V-shaped seed guiding tube, the cross-section varied gradually. A 2-mm baffle plate was incorporated to prevent inlet splashing and to guide the liquid stream along the tube wall. A ramp angle of 120°-160° was evaluated via numerical simulation to ensure optimal flow distribution.

To further investigate the seed transport mechanism, the entire guiding process was divided into three stages: the moment the seed contacts the liquid flow, the seed transport process, and the seeding and landing.

Figure 3 presents a close-up view of the moment the seed contacts the liquid flow. The soybean seed is simplified as a standard sphere. The pressure (p) at any point A (R, θ, φ) in space under the spherical coordinate system is given by Eq. 2:

$$p = p_0 - \rho_g g z - \frac{3}{2}\mu v_w R\left(\frac{R}{r}\right)^2 \cos\theta \tag{2}$$

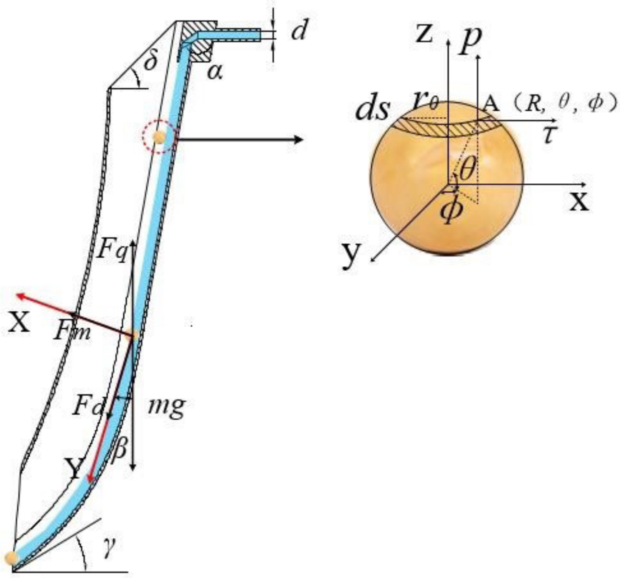

d - Liquid flow inlet diameter, mm; α - Angle of inclined flow channel, °; δ - Liquid inlet angle, °; F_q - Vertical upward buoyancy, N; F_m - Magnus lift from flow field action, N; F_d - Trailing force from positive fluid flow, N; β - Seed guiding angle, °; mg - Gravity of the seed itself, N; γ - Seeding angle, °; θ - Unilateral angle on the seed surface, °; φ - Azimuthal angle on the seed surface, °; ds - Surface area element on the seed, mm²; R - Seed radius, mm; p - Pressure, Pa; and τ - Shearing force, Pa

Figure 3. Working principle of the liquid-flow-assisted seed guiding device

The shearing force (τ) is calculated with Eq. 3:

$$\tau = \frac{3}{2}\frac{\mu v_w}{R}\left(\frac{R}{r}\right)^4 \cos\theta \tag{3}$$

The transformation between Cartesian and spherical coordinates in the pressure equation is z = r cos θ. The z-direction component of the sum was integrated along the entire sphere. Then, the area of the circular portion of the graph was calculated, setting the radius of the circle as r_0, the angle between the circle and the z-axis as θ, the angle between the top and bottom of the circle as dθ, and the corresponding arc length as dh = R dθ. Eq. 4 shows the area of the circle:

$$dS = 2\pi r_0 dh = 2\pi R^2 \sin\theta d\theta \tag{4}$$

Eq. 5 shows the component force in the z-direction generated by p, τ, and the total force on the particle in the z-direction by the fluid:

$$\begin{cases} F_p = \int -p\cos\theta dS = \int_0^\pi -p\cos\theta 2\pi R^2 \sin\theta d\theta = \frac{4}{3}\pi R^3 \rho_g g + 2\pi\mu R v_w \\ F_\tau = \int_0^\pi \tau \sin\theta 2\pi R^2 \sin\theta d\theta = 4\pi\mu R v_w \\ F = F_p + F_\tau = \frac{4}{3}\pi R^3 \rho_g g + 6\pi\mu R v_w \end{cases} \tag{5}$$

where:

F_p - pressure in the z-direction on the seed, N; and,

F_τ - shear force in the z-direction on the seed, N.

Eq. 6 shows the process of energy change in the z-direction after the seed enters the water:

$$\frac{1}{2}mv_0^2 + mg\sin\beta K = \left(F + F_q \sin\beta\right)K + \frac{1}{2}mv_1^2 \tag{6}$$

To ensure that the seed stops bouncing when it contacts the water, the partial velocity (v_1) of the seed in the z-direction when it hits the bottom should be 0, as shown in Eq. 7,

$$\begin{cases} \frac{1}{2}mv_0^2 + mg\sin\beta K < \left(F + F_q \sin\beta\right)K \\ \dfrac{\frac{1}{2}mv_0^2}{\frac{4}{3}\pi R^3 \rho_g g + 6\pi\mu R v_w + F_q \sin\beta - mg\sin\beta} < K \end{cases} \tag{7}$$

where:

β - seed guiding angle, °;
K - depth of liquid flow in the z-direction, mm;
v_w - liquid flow velocity, m s^{-1};
F_q - buoyancy force on the seed, N;
μ - liquid viscosity, Pa·s; and,
ρ_g - liquid density, kg·m^{-3}.

According to Eq. 7, the liquid-flow-assisted seed guiding device is feasible when the liquid within the guiding tube has sufficient depth to provide a buffer for the falling seeds. Therefore, the main factors that affect whether a rebound occurs upon seed-liquid flow contact are the liquid flow velocity (v_w), the initial velocity of the seed (v_0), and the seed guiding angle (β).

Eq. 8 shows force analysis of the seed transport process in the seed guiding tube:

$$\begin{cases} F_X = F_m - mg\sin\beta + F_q \sin\beta \\ F_Y = F_d + mg\cos\beta - F_q \cos\beta \\ F_d = \frac{1}{2}\rho\left(v_w - v_y\right)^2 A_P C_D \\ v_w = \dfrac{Q}{S_T} \\ S_T = \pi r^2 \end{cases} \tag{8}$$

According to D'Alembert's principle, the differential equation for the seed along the direction of motion is shown in Eq. 9:

$$\frac{dv_y}{dt} = \frac{\frac{1}{2}\rho\frac{Q}{S_T} - v_y^2 A_P C_D}{m} + g\cos\beta - \frac{F_q\cos\beta}{m} \tag{9}$$

where:

F_x - force on the seed in the vertical direction of the seed guiding tube, N;
F_y - force on the seed along the curved path of the seed guiding tube, N;
m - seed mass, kg;
g - gravity acceleration, m s^{-2};
ρ - liquid density, m s^{-2};
v_w - liquid velocity, m s^{-1};
v_y - Y-direction velocity of the seed, m s^{-1};
r - radius of the liquid flow inlet, mm;
A_P - area of contact between the seed and liquid flow, m^2;
C_D - coefficient of drag force;
S_T - liquid flow cross-sectional area, m^2; and,
Q - liquid flow rate, mL min^{-1}.

According to Eq. 9, when the seed contacts the liquid stream, the gravity (mg) and buoyancy (F_q) remain unchanged, and acceleration of the seed is affected by the liquid flow rate (Q), the partial velocity of the seed (v_y), and the seed guiding angle (β).

When the seed lands, it is completely separated from the constraints of the seed guiding tube. The seed-liquid flow mixture is expelled from the seed guiding tube, and the seed is surrounded by liquid when it lands. This can provide a buffer for the seed to land on the ground and bounce (Figure 4).

At the seeding point, the force on the seed is mainly gravity (mg) and the support force provided by the seed guiding tube (F). From the perspective of energy conversion, the total energy lost by the seed during the landing process is shown in Eq. 10:

$$\Delta E_P = \frac{1}{2}m\left(v\sin\gamma\right)^2 + \left(mg - F\cos\gamma\right)l \tag{10}$$

where:

γ - angle of seed casting, °; and,
l - height of seed casting, mm.

Based on Eq. 10, in the actual process of seed casting, the energy a seed loses during the landing stage is related to the velocity, casting angle, and height from which the seed falls when it is expelled from the seed guiding tube. Combining the above analyses, the key factors that affect the stability of seed guidance under liquid-flow-assisted conditions are the seed guiding angle (β), the seeding rotation speed (n_p), and the flow rate (Q). A lab-made test bench was used to determine the optimal combination of working parameters of the liquid-flow-assisted seed guiding device. It included a brush-type soybean seed metering device, the liquid-flow-assisted seed guiding device, and the motor and speed controller driving the seed metering device (Figure 5).

The brush-type soybean seed metering device is driven by a motor, while the liquid flow rate in the seed guiding system is regulated by a peristaltic pump. During the experiment, a

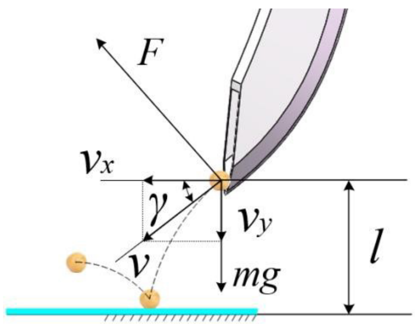

F - Supporting force provided by the seed guide tube, N; v - Exit velocity of the seed, m s^{-1}; v_x and v_y - Horizontal and vertical component velocities of the landing velocity v, m s^{-1}; mg - Gravity of the seed, N; γ - Angle of seed casting, °; and l - Height of seed casting, mm

Figure 4. A schematic diagram of a seed landing

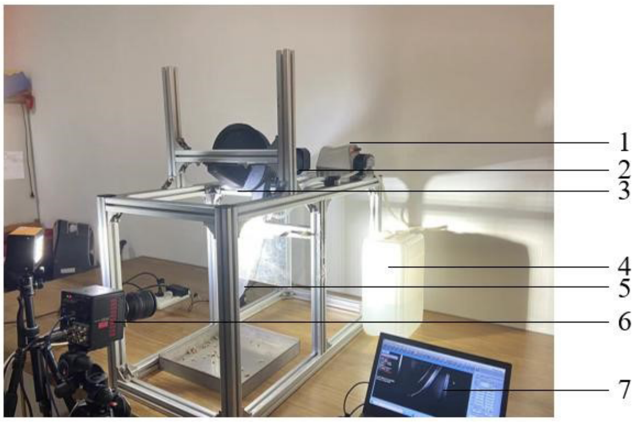

1 - Peristaltic pump; 2 - Motor and governor; 3 - Soybean seed metering device; 4 - Water tank; 5 - Seed guiding tube; 6 - High-speed camera; 7 - Computer

Figure 5. A test bench designed to evaluate the performance of the seed guide tube

high-speed camera recorded the entire process. The number of dispensed seeds and the time interval between adjacent seeds were determined by replaying the video frame by frame. Subsequently, the seed spacing was calculated (Zhang et al., 2023).

Table 1 shows the details of the three-factor, three-level orthogonal test. Each group of tests was repeated three times, and the mean was used for analysis. The values for each parameter were determined based on preliminary experiments: 5°, 10°, and 15° for the seed guiding angle; 26.7, 33.3, and 40.0 rpm, which correspond to a forward speed of 6, 8, and 10 km h^{-1}, respectively, for the rotational speed of the seed metering device; and 600, 800, and 1000 mL min^{-1} for the liquid flow rate (Li et al., 2022).

The test was performed in accordance with the Chinese national standard GB/T6973-2005 protocol for single-grain (precision) planters. One hundred consecutive seeds were randomly selected, and the seed spacing was measured. The test was repeated three times, and the mean was calculated and used for analysis. Two key performance indicators were adopted: the qualified rate of seed spacing (A) and the coefficient of variation of seed spacing (C), as shown in Eqs. 11 and 12, respectively:

$$A = \frac{n_q}{n} \times 100 \quad (11)$$

$$C = \frac{\sigma}{\bar{d}} \times 100 \quad (12)$$

where:

n_q - number of seed spacings that fall within the qualified range;

n - total number of measured seed spacings;

σ - standard deviation of the seed spacings, mm; and,

$\bar{d}$ - mean seed spacing, mm.

Table 1. The experimental factor codes

Code	Seed guiding angle (°)	Seeding rotation speed (rpm)	Flow rate (mL min^{-1})
1	5	26.7	600
0	10	33.3	800
-1	15	40.0	1000

The seed guiding performance of the V-shaped seed guiding tube in the liquid flow-assisted seed guiding device with the optimal combination of operating parameters (a seed guiding angle of 10°, a seeding rotation speed of 33.3 rpm, and a flow rate of 800 mL min^{-1}) was compared with the performance of an ordinary seed guiding tube under different operating speeds. Figure 6 shows a cross-sectional comparison of the two seed guiding tubes. Two key performance indexes were considered: the qualified rate of seed spacing (%) and the coefficient of variation of seed spacing (%).

Figure 6. A cross-sectional comparison of a V-shaped seed guiding tube (left) and an ordinary seed guiding tube (right)

Results and Discussion

Table 2 presents the results of the three-factor, three-level orthogonal test, where X_1 is the seed guiding angle, X_2 is the seeding rotation speed, X_3 is the flow rate of liquid flow, Y_1 is the qualified rate of seed spacing, and Y_2 is the coefficient of variation of seed spacing.

Table 3 presents the analysis of variance (ANOVA) results for the qualified rate of seed spacing. Regression equations for each performance indicator were obtained, as shown in Eq. 13.

$$\begin{aligned} Y_1 &= 1.03X_1 + 5.92X_2 + 0.8112X_3 - \\ &- 0.595X_1X_2 - 0.64X_1X_3 - 0.0775X_2X_3 - \\ &- 3.33X_1^2 - 4.22X_2^2 - 0.6232X_3^2 \end{aligned} \quad (13)$$

Based on ANOVA, the qualified rate of seed spacing was highly significant (F = 11.52, P = 0.0020), while the lack of fit was not significant (F = 0.1229, P = 0.9418). Thus, the regression equation for the model was in accordance with the actual situation.

To study the interaction between multiple factors, one variable was fixed as the median of the interval, and the effect of the other two variables on the indicator was studied, resulting in the response surface in Figure 7.

Table 2. Experimental design and results of orthogonal tests for seed spacing performance with factors of seed guiding angle [X_1], seeding rotation speed [X_2], and flow rate [X_3]

Serial No.	Seed guiding angle (°) X_1	Seeding rotation speed (rpm) X_2	Flow rate (mL min^{-1}) X_3	Qualified rate of seed spacing (%) Y_1	Coefficient of variation of seed spacing (%) Y_2
1	-1	-1	0	76.88	25.55
2	1	-1	0	79.88	25.47
3	-1	1	0	90.66	16.87
4	1	1	0	91.28	15.55
5	-1	0	-1	85.28	24.22
6	1	0	-1	88.87	20.57
7	-1	0	1	88.96	18.98
8	1	0	1	89.99	19.88
9	0	-1	-1	81.33	28.32
10	0	1	-1	92.58	21.26
11	0	-1	1	82.33	26.80
12	0	1	1	93.27	21.30
13	0	0	0	90.23	20.10
14	0	0	0	92.58	19.28
15	0	0	0	96.11	15.55
16	0	0	0	92.66	16.88
17	0	0	0	89.54	17.54

Table 3. Analysis of variance results of qualified rate of seed spacing

Source	Qualified rate of seed spacing Sum of squares	Degree of freedom	Mean square	F	P
Model	430.17	9	47.80	11.5200	0.0020**
X_1	8.49	1	8.49	2.05	0.1958
X_2	280.49	1	280.49	67.59	< 0.0001**
X_3	5.27	1	5.27	1.27	0.2971
X_1X_2	1.42	1	1.42	0.3412	0.5774
X_1X_3	1.64	1	1.64	0.3948	0.5497
X_2X_3	0.024	1	0.024	0.0058	0.9415
X_1^2	46.57	1	46.57	11.22	0.0123*
X_2^2	75.1	1	75.10	18.1	0.0038**
X_3^2	1.64	1	1.64	0.3941	0.5501
Residual	29.05	7	4.15		
Lack of fit	2.45	3	0.82	0.1229	0.9418
Pure error	26.6	4	6.65		
Aggregate	459.22	16			

** $p \le 0.01$; * $p \le 0.05$

As shown in Figures 7A and D, when seeding rotation speed is fixed, the qualified rate of seed spacing increases sharply as the seed guiding angle increases, then tends to stabilise. This trend is due to progressive improvement in seed trajectory control and a reduction in collisions with a larger guiding angle; however, once seed-wall contact has been minimised, increasing the guiding angle confers minimal benefit. Figure 7D indicates that the guiding angle and the rotation speed influence spacing quality independently, rather than synergistically. This observation is consistent with the results reported by Wang et al. (2024), who found that seed tube inclination primarily affects the trajectory alignment, with speed-related effects remaining largely additive in airflow-assisted metering devices.

As shown in Figures 7B and E, when the rotation speed is held constant, the qualified rate remains relatively stable across a liquid flow range of 600-1000 mL min^{-1}. This suggests that even the minimum tested flow provides sufficient buffering to prevent seed-wall collisions, indicating a threshold beyond which additional flow contributes little to performance. The relative plateau in performance further implies that once a stable liquid film is established, it has reached its capacity to dampen seed motion. However, under a fixed flow rate, increasing rotation speed first improves the qualified rate due to more consistent seed delivery, but subsequently causes a slight decline at higher speeds, likely because increased turbulence disrupts the seed trajectory. The mild interaction effect shown in Figure 7E reinforces the idea that while liquid flow stabilises seed descent, its effectiveness is diminished as kinetic energy from high-speed operation exceeds the buffering capability of the film (Baghooee et al., 2023).

As shown in Figures 7C and F, at a constant guiding angle, the qualified rate initially increases as liquid flow increases, reflecting enhanced cushioning of the seed upon impact and a reduction in seed-wall collisions. However, excessive flow may induce turbulence or secondary motion, slightly worsening spacing quality at the highest rate. Conversely, under fixed flow, increasing the guiding angle consistently improves spacing uniformity (Jia et al., 2024). This outcome can be attributed to the role of the guiding angle in stabilising seed trajectory and minimising lateral deflection. The small interaction between the flow rate and the guiding angle indicates that their effects are mainly additive rather than synergistic. The guiding angle contributes to directional stability, while the flow rate primarily enhances dynamic cushioning. These findings emphasise the need to balance structural control and hydrodynamic buffering to achieve optimal seed delivery precision.

The ANOVA results for the coefficient of variation of seed spacing are shown in Table 4. The regression equations for each performance indicator are shown in Eq. 14.

$$\begin{aligned} Y_2 &= -0.5187X_1 - 3.89X_2 - 0.9263X_3 - \\ &- 0.31X_1X_2 + 1.14X_1X_3 + 0.39X_2X_3 - \\ &- 0.2588X_1^2 + 3.25X_2^2 + 3.30X_3^2 \end{aligned} \tag{14}$$

The coefficient of variation of seed spacing was highly significant (F = 8.72, P = 0.0047), while the lack of fit was not significant (F= 0.721, P = 0.5897). Thus, the regression equations fitted to the model were in accordance with the actual situation.

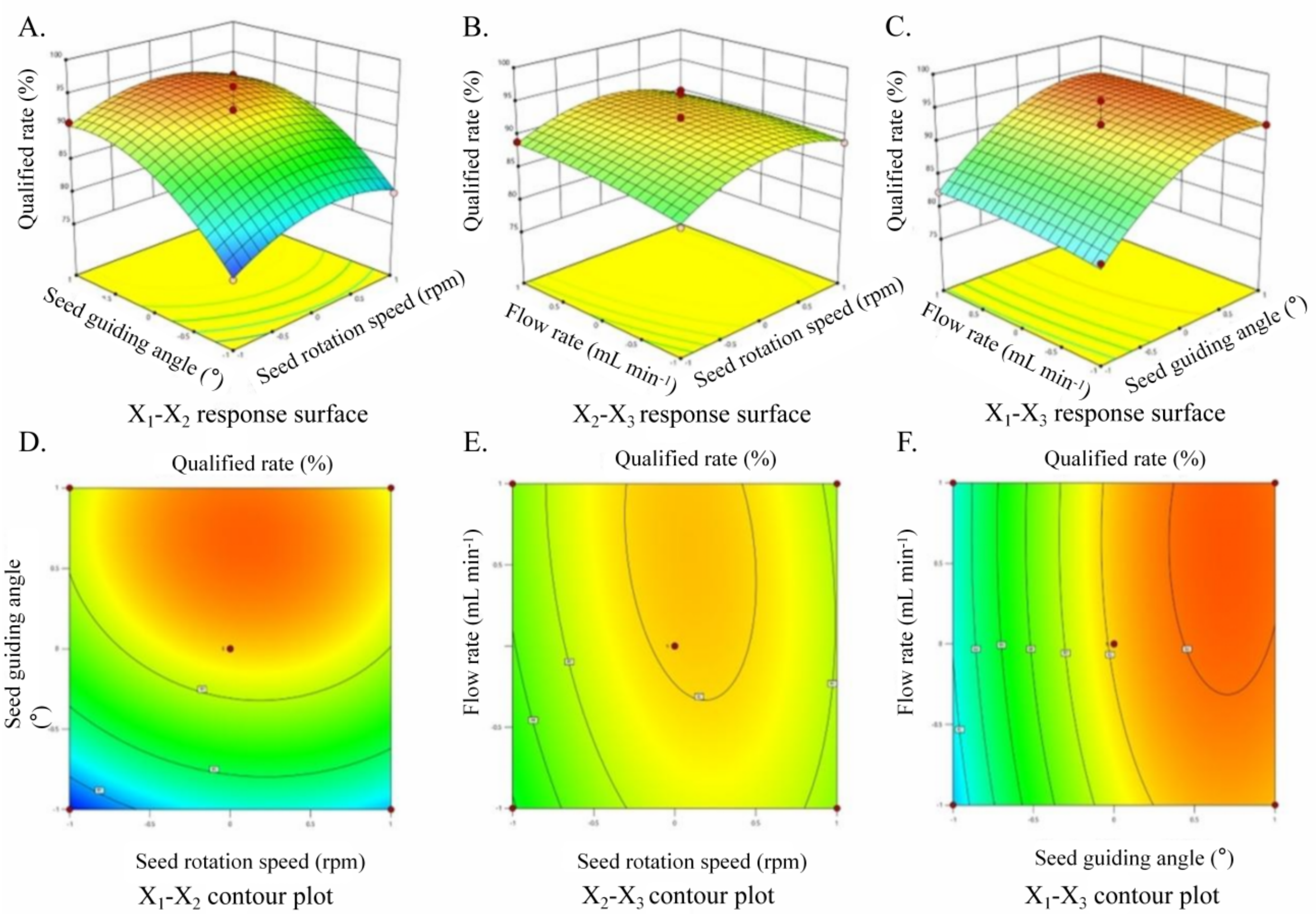

X1-X2 – The response surface represents the interaction between the seed guiding angle (X_1) and the seeding rotation speed (X_2) on the qualified rate (Y_1); X2-X3 – The response surface represents the effect of the interaction between seeding rotation speed (X_2) and the flow rate (X_3) on the qualified rate (Y_1); X1-X3 – The response surface represents the interaction between the seed guiding angle (X_1) and the flow rate (X_3) on the qualified rate (Y_1)

Figure 7. Influence of the seed guiding angle and seed rotation speed on the X_1-X_2 response surface (A and D), the seed rotation speed and flow rate on the X_2-X_3 response surface (B and E), and the seed guiding angle and flow rate on the X_1-X_3 response surface (C and F) of the qualified rate of seed spacing (%)

Table 4. Analysis of variance (ANOVA) of the coefficient of variation of seed spacing

Source	Coefficient of variation of seed spacing			F	P
	Sum of squares	Degree of freedom	Mean square		
Model	231.94	9	25.77	8.72	0.0047**
X_1	2.15	1	2.15	0.7282	0.4217
X_2	121.37	1	121.37	41.05	0.0004**
X_3	6.86	1	6.86	2.32	0.1714
X_1X_2	0.3844	1	0.38	0.13	0.729
X_1X_3	5.18	1	5.18	1.75	0.2274
X_2X_3	0.6084	1	0.61	0.2058	0.6638
X_1^2	0.2819	1	0.28	0.0953	0.7665
X_2^2	44.44	1	44.44	15.03	0.0061**
X_3^2	45.89	1	45.89	15.52	0.0056**
Residual	20.7	7	2.96		
Lack of fit	7.26	3	2.42	0.721	0.5897
Pure error	13.43	4	3.36		
Aggregate	252.64	16			

** $p \leq 0.01$; * $p \leq 0.05$

Next, the interaction between multiple factors was investigated. Specifically, two factors were chosen as variables and another variable was fixed at the median of the interval, resulting in the response surface in Figure 8.

As shown in Figures 8A and D, when the seeding rotation speed is held constant, the coefficient of variation of seed spacing first decreases and then increases as the seed guiding angle increases, indicating the presence of an optimal angle of around 10°. At lower angles, insufficient trajectory control results in more bouncing and lateral deflection, while at excessive angles, the extended seed travel time and increased flow resistance may cause instability or delay. This non-linear trend confirms that moderate guiding angles improve spatial uniformity by stabilising seed descent. In contrast, when the guiding angle remains fixed, increasing the rotation speed leads to a slight but steady decrease in the coefficient of variation, although the overall variation is small. This suggests that while speed influences spacing to a certain degree, its effect is secondary to that of the guiding angle. Moreover, the minimal interaction between these two factors, as shown in Figure 8D, indicates that their influence is largely independent. Li et al. (2024a) reported similarly findings: they observed that geometric factors such as tube inclination are the primary determinants of spacing uniformity, while speed plays a supporting role.

As shown in Figures 8B and E, when the seeding rotation speed is fixed, the coefficient of variation decreases gradually as the liquid flow rate increases, due to enhanced damping effects from a thicker liquid film. The liquid flow reduces the kinetic energy of the seed and suppresses collision-induced variation,

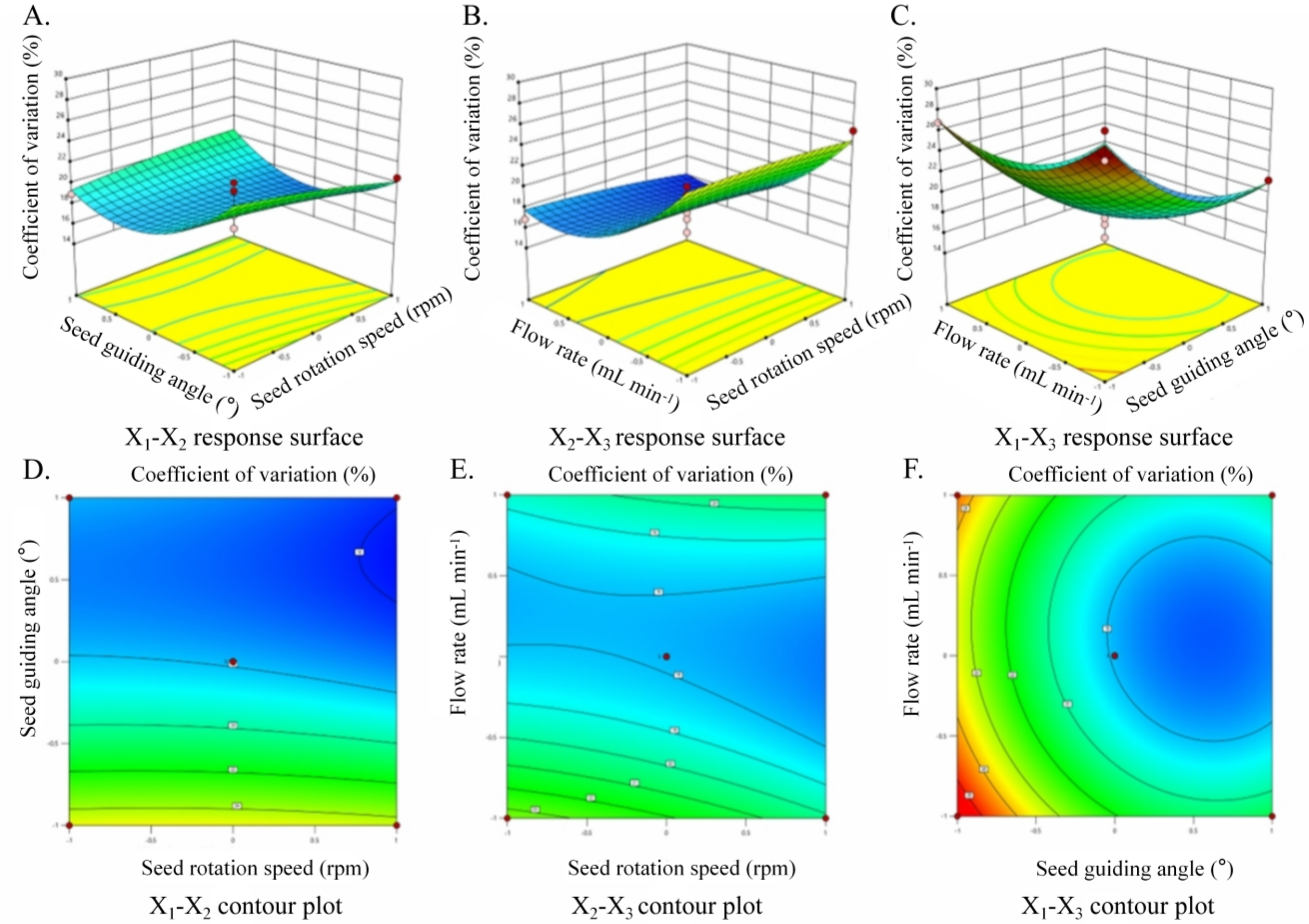

X_1-X_2 – The response surface represents the interaction between the seed guiding angle (X_1) and the seeding rotation speed (X_2) on the coefficient of variation (Y_2); X_2-X_3 – The response surface represents the effect of the interaction between the seeding rotation speed (X_2) and the flow rate (X_3) on the coefficient of variation (Y_2); X_1-X_3 – The response surface represents the interaction between the seed guiding angle (X_1) and the flow rate (X_3) on the coefficient of variation (Y_2)

Figure 8. Influence of the seed guiding angle and the seed rotation speed on the X_1-X_2 response surface (A and D), the seed rotation speed and the flow rate on the X_2-X_3 response surface (B and E), and the seed guiding angle and the flow rate on the X_1-X_3 response surface (C and F) on the coefficient of variation of seed spacing (%)

especially at moderate flow levels. When the liquid flow rate is constant, increasing rotation speed also causes a slight decrease in the coefficient of variation, attributed to more uniform seed discharge intervals. The interaction between these two factors is moderate, as shown in Figure 8E, indicating that higher flow rates can partially compensate for increased dynamic instability at high seeding speeds.

Figures 8C and F demonstrate that when the guiding angle is held constant, the coefficient of variation of seed spacing initially decreases and then slightly increases as the liquid flow rate increases. The initial decrease can be attributed to the formation of a more stable and continuous liquid film along the inner wall of the seed guiding tube, which effectively cushions the seed upon impact and suppresses bouncing, thereby enhancing uniformity. However, as the flow rate continues to rise, the increased liquid velocity induces local turbulence within the tube. This turbulence disrupts the stable descent path of the seed, causing irregular motion and slight deviations, which result in a marginal increase in variation.

Conversely, when the flow rate is fixed, increasing the guiding angle leads to a steady and notable reduction in the coefficient of variation. This occurs because a larger guiding angle alters the seed's trajectory so that it is more aligned with the tube wall, reducing vertical acceleration and limiting the space for lateral deflection. As a result, seeds travel in a more controlled path with reduced collision frequency and more consistent spacing. Consistently, Zhao et al. (2022) demonstrated that optimised structural alignment and angular parameters significantly reduce seed deflection and improve spacing accuracy during descent in precision sowing devices.

Figure 8F shows a negligible interaction between the guiding angle and the flow rate, indicating that their contributions to seed spacing uniformity are independent. This further suggests that while hydrodynamic buffering provided by liquid flow is important, the geometric alignment and mechanical constraint offered by the guiding angle play a more critical role in minimising spacing variation, particularly under high-speed seeding conditions.

In the above analysis, the liquid-flow-assisted seed guiding device achieved its best performance with a seed guiding angle of 10°, a seeding rotation speed of 33.3 rpm, and a liquid flow rate of 800 mL min^{-1}. With these parameters, there was a seed spacing qualified rate of 96.11% and a coefficient of variation of 15.55%. These values reflect a high degree of seed placement uniformity and stability, particularly under simulated high-speed operating conditions (McDonald et al., 2024). This superior performance can be attributed to the synergistic effect of the three optimised parameters. Specifically, the 10° seed guiding angle strikes a balance between providing a sufficient horizontal component to offset forward momentum and minimising seed rebound against the tube wall. Smaller angles reduce control over the trajectory, while larger angles may increase travel time and turbulence. A rotation speed of 33.3 rpm corresponds to a field forward speed of approximately 10 km h^{-1}, representing a practical upper limit in field operations. While lower speeds may further reduce seed interference, they reduce field efficiency. The system's ability to maintain high accuracy at this speed confirms its applicability to modern high-speed planting demands. Finally, the liquid flow rate of 800 mL min^{-1} ensures the formation of a stable liquid film along the seed guiding tube, sufficient to buffer seeds and suppress bouncing, without causing turbulence or washing effects seen at higher flow rates. According to the orthogonal test results, 600 mL min^{-1} provides limited buffering, resulting in occasional seed bouncing, while 1000 mL min^{-1} leads to flow instability and trajectory disturbance due to excessive turbulence (Liu et al., 2023a). Therefore, the effective operating range is 600-1000 mL min^{-1}, with 800 mL min^{-1} representing a well-optimised operating point. This parameter combination outperforms comparable systems in existing research and demonstrates the feasibility and advantage of liquid-assisted seed guiding in high-speed precision sowing.

Finally, the performance of the liquid-flow-assisted seed guiding device under the optimal combination of parameters was compared with the performance of a common seed guiding tube under different operating speeds. Specifically, the seeding rotation speed was used as the experimental factor, set at 20.0, 26.7, and 33.3 rpm, corresponding to a forward speed of 6, 8, and 10 km h^{-1}, respectively. The performance was assessed based on the qualified rate of seed spacing (%) and the coefficient of variation of seed spacing (%). Table 5 presents the results for each device.

For both devices, as the rotation speed increased, the qualified rate of seed spacing decreased while the coefficient of variation increased, suggesting that higher rotational speeds negatively affect seed placement accuracy due to increased seed bouncing and instability of the seed trajectory. Consistently, Yang et al. (2022) observed that seeding at higher speeds increases the miss index and spacing variation. Wei et al. (2022) demonstrated that increased seeding speed exacerbates seed collisions within the delivery system, reducing uniformity. This trend indicates decreased spacing uniformity at higher speeds due to increased seed interference and collisions during descent. However, under all tested conditions, the liquid-flow-assisted device consistently outperformed the conventional tube.

At the highest seeding speed (33.3 rpm), the qualified rate with the liquid-assisted device was 91.06%, compared with 83.36% for the ordinary tube. Similarly, the coefficient of variation was reduced from 27.86 to 16.88%, showing significantly improved uniformity. This improvement is attributed to the liquid film inside the V-shaped guiding tube, which cushions the seeds, reduces bouncing, and stabilises the descent trajectory. In contrast, the ordinary tube lacks this buffering effect, so seeds are more prone to rebound and deviation due to direct mechanical contact with the tube wall. The liquid medium also helps maintain consistent speed and orientation, especially under high-speed operation. Overall, the liquid-assisted seed guiding device effectively mitigates the negative effects of high-speed seeding. It improves seed placement accuracy by increasing the qualified rate of seed spacing by 7.7% and reducing the coefficient of variation by 10.98%, providing clear advantages over traditional designs.

Conclusion

1. A liquid flow-assisted seed guiding device was designed to reduce seed collisions in the seed guiding tube by utilising forward liquid flow, thereby improving plant spacing uniformity. Analysis of seed movement revealed that the seed guiding angle, the seeding rotation speed, and the liquid flow rate are the main factors that affect sowing performance.

2. The multifactor experimental results showed that the best seed distribution uniformity and stability were achieved at a seed guiding angle of 10°, a seeding rotation speed of 33.3 rpm, and a flow rate of 800 mL min^{-1}. Under these conditions, the qualified rate of seed spacing was 96.11% and the coefficient of variation of seed spacing was 15.55%.

3. Compared with a conventional seed guiding tube, at a forward speed of 10 km h^{-1}, the liquid flow-assisted seed delivery device achieved a seed spacing qualified rate of over 92%, with a 7.7% increase in seed spacing qualified rate and a 10.98% decrease in coefficient of variation compared with the traditional device.

Contribution of authors: Xiaomeng Xia: research advisor, data analysis, conceptualization of the problem, preparation of the manuscript, and literature review. Jian Wang: research, data acquisition, data analysis, implementation of computational simulations, drafted the manuscript, preparation of the manuscript and literature review. Jinhui Zhao: data analysis, review, and drafted the manuscript. Mingwei Li: supervision of the work, administration.

Data availability statement: The authors declare that there are no data underlying the text.

Conflict of interest: The authors declare no conflict of interest.

Financing statement: There was no source of funding for the research.

Table 5. Comparative validation test under different operating speeds

Seeding rotation speed (rpm)	Forward speed (km h^{-1})	Ordinary seed guiding tube		Liquid flow-assisted seed guiding device	
		Qualified rate of seed spacing (%)	Coefficient of variation of seed spacing (%)	Qualified rate of seed spacing (%)	Coefficient of variation of seed spacing (%)
20.0	6	92.21	25.55	95.37	12.28
26.7	8	86.25	25.47	92.78	14.55
33.3	10	83.36	27.86	91.06	16.88

Acknowledgement: This work was supported by the Natural Science Foundation of Shandong Province (ZR2024QE004), the High-quality Development Project for the Ministry of Industry and Information (2023ZY02009), the Youth Innovation Team Development Plan of Universities of Shandong Province (2022KJ225), and the Opening Fund of the State Key Laboratory of Agricultural Equipment Technology (NKL-2023-010).

Literature Cited

Baghooee, M.; Karparvarfard, S. H.; Azimi-Nejadian, H.; Keramat-Jahromi, M.; Balanian, H.; Sardarpour, F. DEM simulation for seeding performance of a slotted roller seed-metering device for planting maize in laboratory condition. Journal of Biosystems Engineering, v.48, p.428-436, 2023. https://doi.org/10.1007/s42853-023-00202-z

Carpes, D. P.; Alonco, A. D.; Rossato, F. P. Effect of different conductor tubes on the longitudinal distribution of corn seeds. Revista Brasileira de Engenharia Agrícola e Ambiental, v.21, p.657-662, 2017. https://doi.org/10.1590/1807-1929/agriambi.v21n9p657-662

Chen, Y. L.; Han, J.; Lan, Y. B.; Zhang, M.; Jin, Y. C.; Zhang, Z.; Wang, W. J. Design and experiment of a combined seed guide tube for precision seed metering device. Transactions of the Chinese Society of Agricultural Engineering, v.38, p.14-24, 2022. https://doi.org/10.11975/j.issn.1002-6819.2022.24.002

Chen, Y. L.; Jing, H. R.; Zhang, Z.; Guo, Y. H.; Ning, X. F. Design and experiment of the key components of the seeding monomer for high-speed corn no-till seeders. International Journal of Agricultural and Biological Engineering, v.16, p.95-103, 2023. https://doi.org/10.25165/j.ijabe.20231605.7687

Dong, J. X.; Gao, X. J.; Zhang, S. L.; Huang, Y. X.; Zhang, C.; Shi, J. T. Design and experiment of maize attitude-control guided seed metering device and seed guiding mechanism. Transactions of the Chinese Society for Agricultural Machinery, v.54, p.25-34, 2023. https://doi.org/10.6041/j.issn.1000-1298.2023.10.002

Endrerud, C. H. Influence of tube configuration on seed delivery to a coulter. Journal of Agricultural Engineering Research, v.74, p.177-184, 1999. https://doi.org/10.1006/jaer.1999.0449

Gai, M. M.; Yang, J.; Li, X. H.; Qu, Z.; Li, H.; Yu, Y. C. Design and test of guided horizontal disc soybean precision seeder. Jiangsu Agricultural Sciences, v.51, p.200-206, 2023. https://doi.org/10.15889/j.issn.1002-1302.2023.22.027

Hou, S. Y.; Zou, Z.; Wei, Z. P.; Zhu, Y. F.; Chen, H. T. Design and experiment of flexible mechanical soybean precision seed-metering device. Transactions of the Chinese Society for Agricultural Machinery, v.51, p.77-86, 2020. https://doi.org/10.6041/j.issn.1000-1298.2020.10.010

Jia, X.; Zhu, J. Y.; Guo, G.; Huang, Y. X.; Gao, X. J.; Zhang, C. Q. Design and test of a novel converging groove-guided seed tube for precision seeding of maize. Biosystems Engineering, v.245, p.36-55, 2024. https://doi.org/10.1016/j.biosystemseng.2024.06.012

Kocher, M. F.; Coleman, J. M.; Smith, J. A.; Kachman, S. D. Corn seed spacing uniformity as affected by seed tube condition. Applied Engineering in Agriculture, v.27, p.177-183, 2011. https://doi.org/10.13031/2013.36484

Kumar, R.; Raheman, H. Detection of flow of seeds in the seed delivery tube and choking of boot of a seed drill. Computers and Electronics in Agriculture, v.153, p.266-277, 2018. https://doi.org/10.1016/j.compag.2018.08.035

Li, F. X.; Tang, K. Y.; Ge, Y. F.; Yang, D. F.; Li, D. Z.; Ma, J. J. Research on optimal design method of maize seed tube based on DEM. Journal of Chinese Agricultural Mechanization, v.45, p.41-47, 2024a. https://doi.org/10.13733/j.jcam.issn.2095-5553.2024.02.007

Li, Q. C.; Feng, J. L.; Jiang, W. Design and experiment on precision seed metering device for narrow-row and dense planting of soybean. INMATEH-Agricultural Engineering, v.67, e353, 2022. https://doi.org/10.35633/nmateh-67-36

Li, Y. F.; Zhou, W. Q.; Ma, C. C.; Feng, Z. H.; Wang, J. W.; Yi, S. J.; Wang, S. Design and optimization of the seed conveying system for belt-type high-speed corn seed guiding device. International Journal of Agricultural and Biological Engineering, v.17, p.123-131, 2024b. https://doi.org/10.25165/j.ijabe.20241702.8427

Liao, Y. T.; Li, C. L.; Liao, Q. X.; Wang, L. Research progress of seed guiding technology and device of planter. Transactions of the Chinese Society for Agricultural Machinery, v.51, p.1-14, 2020. https://doi.org/10.6041/j.issn.1000-1298.2020.12.001

Liu, H. Z.; Li, Z. Y.; Wang, C.; Zhang, Q. S. Impacts of inflow conditions on the measurement stability of a turbulence-mitigation based liquid concentration detection system. Flow Measurement and Instrumentation, v.90, 2023a. https://doi.org/10.1016/j.flowmeasinst.2023.102337.

Liu, R.; Liu, Y. Q.; Liu, Z. J.; Liu, L. J. Study on positive pressure airflow-assisted seed guide device for high-speed precision maize planter. Transactions of the Chinese Society for Agricultural Machinery, v.54, p.156-166, 2023b. https://doi.org/10.6041/j.issn.1000-1298.2023.07.015

McDonald, G. K.; Minkey, D.; Desbiolles, J.; Clarke, G.; Allen, R.; Noack, S.; Schmitt, S.; Amougis, A. Responses to precision planting in canola and grain legume crops. Field Crops Research, v.315, e109451, 2024. https://doi.org/10.1016/j.fcr.2024.109451

Ren, D. L.; Liu, T.; Xia, S. H.; Chen, Y. X.; Wang, W. W.; Li, Z. D. Design and seed filling performance test of cavity plate combination hole type seeding plate for corn and soybean. Transactions of the Chinese Society for Agricultural Machinery, v.55, p.73-89, 2024. https://doi.org/10.6041/j.issn.1000-1298.2024.02.007

Wang, L.; Cong, J. L.; Ren, N.; Ying, J. C.; Wang, X. D.; Liao, Y. T.; Liao, Q. X. Influence of surface slope on the seeding performance of air-assisted centralized metering device for rapeseed based on numerical simulation. Computers and Electronics in Agriculture, v.218, e108734, 2024. https://doi.org/10.1016/j.compag.2024.108734

Wang, L.; Qiu, L. C.; Li, Y. K. High-speed photography analysis on process of corn seeds moving in seed tube. Journal of Agricultural Mechanization Research, v.32, p.130-132, 2010. https://doi.org/10.13427/j.cnki.njyi.2010.10.016

Wei, M. J.; Diao, P. S.; Wang, W. J. Design and experiment of the seed delivery device with a rotating brush wheel for precision seeder. Engenharia Agrícola, v.42, e20220089, 2022. https://doi.org/10.1590/1809-4430-Eng.Agric.v42n6e20220089/2022

Xue, P.; Hao, Y. J.; Jiao, W.; Ren, J.; Yang, F. F.; Ren, D.; Zhang, W. H.; Rong, H.; Hu, B.; Huang, Y. X. Design and test of a double-curved guiding groove for a high-speed precision seed-metering device. Transactions of the ASABE, v.63, p.1349-1360, 2020. https://doi.org/10.13031/trans.13331

Yang, S.; Zhai, C. Y.; Gao, Y. Y.; Dou, H. J.; Zhao, X. G.; He, Y. K.; Wang, X. Planting uniformity performance of motor-driven maize precision seeding systems. International Journal of Agricultural and Biological Engineering, v.15, p.101-108, 2022. https://doi.org/10.25165/j.ijabe.20221505.5911

Yazgi, A. Effect of seed tubes on corn planter performance. Applied Engineering in Agriculture, v.32, p.783-790, 2016. https://doi.org/10.13031/aea.11274

Zhang, J. C.; Hou, Y. H.; Ji, W. Y.; Zheng, P.; Yan, S. C.; Hou, S. Y.; Cai, C. Evaluation of a real-time monitoring and management system of soybean precision seed metering devices. Agronomy, v.13, e541, 2023. https://doi.org/10.3390/agronomy13020541

Zhao, H. H.; Zhang, D. X.; Yang, L.; Cui, T.; Song, W.; He, X. T.; Wu, H. L.; Dong, J. Q. Optimal design and experiment of critical components of hand-pushing corn plot precision planter. Agriculture, v.12, e2103, 2022. https://doi.org/10.3390/agriculture12122103

Zhu, H. B.; Wu, X.; Bai, L. Z.; Li, R. D.; Guo, G. Y.; Qin, J.; Zhang, Y. Y.; Li, H. Design and experiment of a soybean shaftless spiral seed discharge and seed delivery device. Scientific Reports, v.13, e20751, 2023. https://doi.org/10.1038/s41598-023-48117-1